

無し

G. 研究発表

1. 論文発表

1. 平塚純一, 栗飯原輝人, 小野公二

【粒子線治療の普及に向けた課題と展望】ホウ素中性子捕捉療法(BNCT)の現状と可能性 さらなる展開に向けた課題はなにか(解説/特集)
DIGITAL MEDICINE(1345-3351)7巻6号 Page28-30(2009.05)

2. 学会発表

1. 栗飯原輝人, 平塚純一, 宇野雅子, 小野公二, 熊田博明, 原田保

ホウ素中性子捕捉療法の頭頸部癌に対する有効性の検討 先進医療に向けて
第110回 日本耳鼻咽喉科学会総会・学術講演会 2009.05.14-16 東京
日本耳鼻咽喉科学会会報(0030-6622)112巻4号 Page363(2009.04)

2. 栗飯原輝人, 平塚純一, 宇野雅子, 小野公二, 原田保

進行頭頸部癌に対する原子炉硼素中性子捕捉療法: 加速器硼素中性子捕捉療法に向けて
第33回日本頭頸部癌学会 2009.06.11-13 札幌
頭頸部癌(1349-5747)35巻2 Page137(2009.05)

3. 栗飯原輝人, 平塚純一, 宇野雅子, 小野公二, 原田保

頭頸部癌に対する原子炉ホウ素中性子捕捉療法
第71回耳鼻咽喉科臨床学会総会 2009.07.02-03 旭川
耳鼻咽喉科臨床(0032-6313)補冊124 Page165(2009.06)

4. 平塚純一

BNCT 総論1-臨床
日本放射線腫瘍学会第22回学術大会 2009.9.17-19 京都
日本放射線腫瘍学会誌 21Suppl.1 96 2009

5. 栗飯原輝人, 平塚純一, 森田倫正, 宇野雅子, 小野公二, 原田保

頭頸部癌に対する原子炉ホウ素中性子捕捉療法
第47回日本癌治療学会学術集会 2009.10.22-24 横浜
日本癌治療学会誌(0021-4671)44巻2号 Page516(2009.09)

H. 知的財産権の出願・登録状況

(予定を含む。)

1. 特許取得

無し

2. 実用新案登録

無し

3. その他

無し

分担研究報告書

「簡便なホウ素濃度測定技術の開発と組織内ホウ素濃度分布の検索」

切畑光統 大阪府立大学大学院・教授

研究要旨

中皮腫BNCTのホウ素薬剤として実用が期待されるBPAおよびBSHの濃度と動態を簡便に把握するための測定方法を研究開発した。共存するBPAとBSHの著しく異なる血中濃度を、同時に個別定量するために、最適化された4E3（抗BPA抗体）およびA9H3（抗BSH抗体）をマウス免疫により作製した。これらを用いたELISAにより、高濃度BPAと比較的低濃度のBSHが共存するサンプルを、一回の希釈操作（前処理）で、同じプレート上で定量分析する事に成功した。

A. 研究目的

血中ホウ素薬剤の個別濃度を簡便に測定する分析法および組織内分布の評価法を開発する。

B. 研究方法

血中BPAおよびBSH濃度の分別定量は、抗BPA抗体および抗BSH抗体を用いた酵素免疫抗体（ELISA）法により行なう。また、組織内動態は ^{18}F -BPA/PET および ^{18}F -BSH/PET 法を開発して行なう。

（倫理面への配慮）

大阪府立大学動物実験委員会規定に基づき、同委員会の認可の下でマウスによる抗体作製を行なった。

C. 研究結果

共存するBPAとBSHの著しく異なる血中濃度を、同時に個別定量するために、最適化された4E3（抗BPA抗体）およびA9H3（抗BSH抗体）をマウス免疫により作製した。これらを用いたELISAにより、高濃度BPAと比較的低濃度のBSHが共存するサンプルを、一回の希釈操作（前処理）で、同じプレート上で定量分析する事に成功した。再現性を示す変動値（CV）は4-11%であった。また、分析に要した時間は約40分であった。現在、マイクロ流路式ELISAシステムによる分析時間の短縮化を検討している。

未開拓の ^{18}F -BSH/PET を実現するためのトレーサーとして、 ^{18}FMe -BSH および ^{18}FET -BSHを分子設計し、Fによる置換反応を鍵反応とする合成方法を考案した。これらのコールド体（ ^{19}F 体）を当面の標的化合物として、合成経路の確立と反応条件の最適化を行なっている。

D. 考察

ELISA法により、濃度の異なる2つのホウ素薬剤を同時に、且つ、簡単な前処理操作で分別定量するためには、高い交差反応性と同時に、抗原結合能が異なる2種の抗体を作製する事が必要であった。本実験で新たに作製した4E3は、BPAに対する高い構造認識能と弱い結合力を同時に具備し、安定で本分析に最適の抗体であった。

加速器による ^{18}F の製造工程とその半減期（約2時間）を考慮すれば、PETトレーサーとしての ^{18}FMe -B

SH および¹⁸FEt-BSH は、ホットルームに於いて、対応するプロモ体から F による置換反応により誘導する事が最も合理的であると考えられる。

E. 結論

本研究で開発したELISA法は、サンプルの前処理が簡単で、再現性の高い測定方法であるが約40分間を要した。臨床の現場に適用するには、この系を高分子ビーズを担体とするマイクロELISA法に応用し、分析時間の短縮化を図ることが重要である。¹⁸FMe-BSH および¹⁸FEt-BSH は、未開発のBSH/PETトレーサーとして有望であると考えられるが、今後、合成方法や生体内挙動の更なる精査を必要とする。

G. 研究発表

1. 論文発表

1. Feng B, Tomizawa K, Michiue H, Miyatake S, Han XJ, Fujimura A, Seno M, Kirihata M, Matsui H, Delivery of sodium borocaptate to glioma cells using immunoliposome conjugated with anti-EGFR antibodies by ZZ-His. *Biomaterials*. 30 (9), 1746-1755, 2009
2. Tanimori S, Nishimura T, Kirihata M, Synthesis of novel quinoxaline derivatives and its cytotoxic activities. *Bioorg Med Chem Lett*. 19 (15), 4119-4121, 2009

2. 学会発表

第7回日本中性子捕捉療法学会学術大会(平成22年8月6-7日、於 学習院大学)において発表の予定。

H. 知的財産権の出願・登録状況

(予定を含む。)

1. 特許取得

BSH/PETトレーサーの特許申請を準備中。

分担研究報告書

「肺における中性子分布の改善と照射技術の改良の研究」

櫻井良憲 京都大学原子炉実験所・准教授

研究要旨

悪性胸膜中皮腫に対するホウ素中性子捕捉療法 (BNCT) の高度化のために、中性子束分布改善および照射技術改良について検討を行っている。これに関連して、当該年度は、(1) BNCT用照射場の特性評価、(2) BNCT用線量評価手法の検討、(3) 胸膜中皮腫BNCTに関するシミュレーション、を行った。

A. 研究目的

本分担では、悪性胸膜中皮腫に対するホウ素中性子捕捉療法 (BNCT) の高度化について、物理工学的な面から検討を行っている。特に、中性子束分布の改善および照射技術の改良に重点を置き、照射ビームの中性子エネルギー、方向性、照射野の大きさ、等に関する最適化を行うことを目的としている。当該年度は、BNCT臨床に利用されている京都大学研究炉”KUR”の運転が休止していたことと、京都大学原子炉実験所内に新たに設置されたサイクロトロンベース熱外中性子源”C-BENS”の特性データ評価が開始されたことを踏まえて、悪性胸膜中皮腫BNCTのために必要となる基礎データの評価および再評価を中心に行うこととした。併せて、悪性胸膜中皮腫BNCTの線量評価手法に関する検討も行った。さらに、胸膜中皮腫BNCTにおける中性子束分布改善および照射技術改良について、簡単なシミュレーションを行った。

B. 研究方法

当該年度はKURの運転が休止していたことと、C-BENSの利用に制限があったことから、シミュレーション計算を主体に進めた。

(1) BNCT用照射場の特性評価：主に、2008年10月に京都大学原子炉実験所に設置されたサイクロトロンベース熱外中性子源”C-BENS”に関する照射特性評価を行った。フリーインエアでのコリメータ出口における照射特性と、BNCT臨床を想定したファントム内での線量分布特性の評価を行った。中性子束については、金箔、インジウム箔、アルミニウム、箔等を用いた放射化箔方により評価した。 γ 線線量率については、熱ルミネッセンス線量計 (TLD) を用いて測定した。また、多重電離箱を用いて、中性子および γ 線の吸収線量率の評価も行った。

(2) BNCT用線量評価手法の検討：主に、「多重即発 γ 線テレスコープシステム」と「QA用ファントム」に関する可能性検討を行った。「 γ 線テレスコープシステム」は、従来、肝腫瘍BNCTにおける線量評価のために設置したものであり、生体中の組織に含まれる水素と中性子との反応により発生する2.22MeVの即発 γ 線と、投与した薬剤注の硼素10と中性子との反応により発生する478keVの即発 γ 線を計数することで、照射時の硼素10濃度を定量化するためのものである。硼素10の代わりに多数の即発 γ 線を発生するGd等を利用することで、濃度だけでなく、位置に関する情報も得られる可能性がある。「QAファントム」に関しては、検出器の性能の限界により困難であった中高エネルギー中性子に関する線量評価を、ファントムの材質の工夫により改善することを目指している。低エネルギー中性子に対して吸収の大きいリチウム6を適度に水等のファントム材に混ぜることで、中高エネルギー中性子の分布を際立たせる

ことを考えている。QAファントムに関するシミュレーションは、モンテカルロコード”MCNP”を用いて行った。

(3) 胸膜中皮腫BNCTに関するシミュレーション：CT等の診断画像をもとに、悪性胸膜中皮腫を想定した体系を作成し、シミュレーション計算を行った。KURに付属するBNCT用中性子照射場「重水中性子照射設備」の熱中性子照射モード、混合中性子照射モード、熱外中性子照射モードの3種類の線質のビームを線源として与えた。シミュレーション計算には、京都大学においてBNCT時の線量計画に用いているコードシステム”SERA”を用いた。二次元線量分布およびDose Volume Histogram (DVH)を比較することで、中性子ビームのエネルギーに関する評価を行った。また、多方向照射に関する簡単なシミュレーションも行った。

C. 研究結果

(1) BNCT用照射場の特性評価：フリーインエアにおけるC-BENSの照射特性としては、熱外中性子ビーム強度がKURのものに比べて、2倍近く改善されていることが確認された。混在する高エネルギー中性子および γ 線については、C-BENSの方が数倍程度、KURのものに比べて大きかった。これら混在成分の低減のための対策を現在行っているところである。ファントム内の分布については、C-BENSの方がKURよりも硼素10による線量分布の平坦度は増していることが確認された。一方で、ファントム内でも、高エネルギー中性子とおよび γ 線等の混在成分の寄与が大きく、実質的な相対分布としてはKURに近いものになると考えられる。

(2) BNCT用線量評価手法の検討：「多重即発 γ 線テレスコープシステム」については、その有効性が確認された。エネルギーの異なる γ 線の発生分布状況が得られることで、硼素10と中性子との反応分布が評価できる可能性が示された。当該年度は、従来のシステムとの比較のため、肝腫瘍を対象にした検討のみしか行っていないが、中皮腫等の肺癌についても適用可能である。動きや変形の大きい肺を対象としたBNCTにおいては、このシステムは有力な線量評価ツールになると考えられる。「QAファントム」についても、ファントム材中に混ぜるリチウム6の濃度を変えることで、中高エネルギーの中性子の分布状況が評価できることが示された。95%に濃縮したリチウム6を水酸化リチウムとして10%程度水に混ぜることで、高エネルギー中性子のみによる線量分布を評価できることが確認された。

(3) 胸膜中皮腫BNCTに関するシミュレーション：二次元線量分布およびDVH両方から判断して、中皮腫が肺全体に及ぶ場合、熱外中性子ビームによるBNCTが最も有効であることが確認された。比較的表層部に患部が集中している症例については、熱あるいは混合照射の方が有効であることが示された。身体を中心付近の患部については、熱外中性子照射でも線量不足になることは避けられないため、多方向照射が必要となると結論づけられた。

D. 考察

本分担の主テーマとなっている胸膜中皮腫BNCTに関する中性子束分布改善および照射技術改良について考察する。結果に示したように、胸膜中皮腫についても、脳腫瘍と同様に、熱外中性子照射が最適であることが確認された。しかしながら、胸膜中皮腫が左右両方の肺全体にわたり分布している状況を考えると、熱外中性子ビームを用いても単方向照射だけでは腫瘍全体に治癒線量を与えることは困難であり、多方向照射が必要不可欠ということになる。また、生体内での中性子減衰の観点から、大面積での照射が望ましい。大面積多方向照射は腫瘍全体に与える線量を増加することになるが、一方で正常部位に与える線量も増加し、特に、照射と照射のオーバーラップ箇所に耐用線量以上の線量を与えてしまう可能性も懸念される。治癒線量の均一化、および、正常組織でのピーク線量低減、の2つの観点から照射技術の改良を検討することが重要である。

E. 結論

京都大学原子炉実験所では、近い将来、従来のKURに加えて、C-BENSにおいてもBNCTが行われる予定で

あり、その対象として胸膜中皮腫も含まれている。上述のようにC-BENSはKURよりも、線質面では若干落ちるが、生体内で得られる硼素10の反応分布については、特に深部で改善されている。このことから、C-BENSにおける胸膜中皮腫BNCTでは、KUR以上の治癒効果が期待できる。BNCTの理想的な照射手法は、患部全体に全方向から中性子照射を行い、硼素10と反応する熱中性子分布を平坦化することにある。今後は、この観点から、胸膜中皮腫BNCTにおける付与線量の平坦化、均一化について検討を進める予定である。また、実際の臨床を目標に、両設備の照射特性データ評価をより詳細に進めるとともに、線量評価手法の高度化も目指す予定である。

F. 健康危険情報 (あれば記入下さい)

特に無し。

G. 研究発表

1. 論文発表

特に無し。

2. 学会発表

- 1) 櫻井良憲, 田中浩基, 鈴木 実, 菓子野元郎, 劉 勇, 木梨友子, 増永真一郎, 丸橋 晃, 小野公二, 「BNCTのための多重即発 γ 線テレスコープシステムの可能性検討」, 第44京大原子炉実験所学術講演会 (2010.1) 熊取。
- 2) 田中浩基, 櫻井良憲, 丸橋 晃, 鈴木 実, 増永慎一郎, 菓子野元郎, 劉 勇, 木梨友子, 小野公二, 密本俊典, 矢島 暁, 筒井裕士, 佐藤岳実, 高田真志, 浅野智之, 「硼素中性子捕捉療法のためのサイクロトロンベース熱外中性子源のビーム特性」, 日本原子力学会 2010年春の年会 (2010.3) 水戸。
- 3) 上田治明, 櫻井良憲, 田中浩基, 丸橋 晃, 小野公二, 「ボナーボールを用いたサイクロトロンベース BNCT 用熱外中性子照射場のスペクトル評価」, 日本医学物理学会 第99回学術大会 (2010.4) 横浜。
- 4) 田中浩基, 櫻井良憲, 鈴木 実, 増永慎一郎, 密本俊典, 矢島 暁, 高田真志, 浅野智之, 小野公二, 丸橋 晃, 「サイクロトロンベース熱外中性子源のためのターゲットからの中性子スペクトル測定」, 日本医学物理学会 第99回学術大会 (2010.4) 横浜。
- 5) 藤井孝明, 櫻井良憲, 田中浩基, 丸橋 晃, 小野公二, 「BNCT 用多重電離箱システムに関する検討 (2) サイクロトロンベース熱外中性子照射場に対する電離箱の最適化」, 日本医学物理学会 第99回学術大会 (2010.4) 横浜。
- 6) 櫻井良憲, 藤井孝明, 田中浩基, 鈴木 実, 劉 勇, 菓子野元郎, 木梨友子, 増永慎一郎, 小野公二, 丸橋 晃, 「硼素中性子捕捉療法における QA 用ファントムに関する検討」, 日本医学物理学会 第99回学術大会 (2010.4) 横浜。

H. 知的財産権の出願・登録状況

(予定を含む。)

1. 特許取得

特に無し。

2. 実用新案登録

特に無し。

3. その他

特に無し。

研究成果の刊行に関する一覧表

書籍

著者氏名	論文タイトル名	書籍全体の 編集者名	書籍名	出版社名	出版地	出版年	ページ
中野孝司	胸膜中皮腫、がん薬物療 法学—基礎・臨床研究の アップデート		日本臨床			2009	629-634
中野孝司	悪性中皮腫の臨床病態		Medical Technology			2009	191-195
中野孝司	悪性胸膜中皮腫(びまん 性悪性胸膜中皮腫)		別冊日本臨床			2009	380-384
中野孝司	胸膜線維性腫瘍(良性限 局型胸膜中皮腫)		別冊日本臨床			2009	398-401
中野孝司	悪性胸膜中皮腫、胸膜炎 を疑うとき、プライマ リ・ケアに必要な画像診 断のコツ		診断と治療			2009	178-186
中野孝司	良性アスベスト関連疾 患の胸部画像所見は中 皮腫高罹患リスクの指 標か?		肺癌			2009	78-82
中野孝司	悪性胸膜中皮腫 講座 ピットホール		呼吸			2009	509-515
中野孝司	切除可能悪性胸膜中皮 腫に対するペメトレキ セドを含む集学的治療 に関する妥当性試験.		肺癌			2009	403-408
中野孝司	胸膜中皮腫に対する集 学的治療に向けて.		肺癌			2009	392-396
中野孝司	悪性胸膜中皮腫を対象 としたLY231514とシス プラチン併用療法の安 全性情報収集のための		肺癌			2009	988-993

雑誌

発表者氏名	論文タイトル名	発表誌名	巻号	ページ	出版年
G. KASHINO, S. FUKUTANI, M. SUZUKI, Y. LIU, K. NAGATA, S. MASUNAGA, A. MARUHASHI, H. TANAKA, Y. SAKURAI, Y. KINASHI, N. FUJII, K. ONO	A Simple and Rapid Method for Measurement of ^{10}B - <i>para</i> -Boronophenylalanine in the Blood for Boron Neutron Capture Therapy Using Fluorescence Spectrophotometry.	J Radiat Res	50	377-382	2009
H. Tanaka, Y. Sakurai, M. Suzuki, S. Masunaga, Y. Kinashi, G. Kashino, Y. Liu, T. Mitsumoto, S. Yajima, H. Tsutsui, A. Maruhashi, K. Ono	Characteristics comparison between a cyclotron-based neutron source and KUR-HWNIF for boron neutron capture therapy.	Nuclear Instruments and Methods in Physics Research B	267	1970-1977	2009
M. Suzuki, H. Tanaka, Y. Sakurai, G. Kashino, Y. Liu, S. Masunaga, Y. Kinashi, T. Mitsumoto, S. Yajima, H. Tsutsui, T. Sato, A. Maruhashi, K. Ono	Impact of accelerator-based boron neutron capture therapy (AB-BNCT) on the treatment of multiple liver tumors and malignant pleural mesothelioma.	Radiotherapy & Oncology.	92	89-95	2009
H. Tanaka, Y. Sakurai, M. Suzuki, T. Takata, S. Masunaga, Y. Kinashi, G. Kashino, Y. Liu, T. Mitsumoto, S. Yajima, H. Tsutsui, M. Takada, A. Maruhashi, K. Ono	Improvement of dose distribution in phantom by using epithermal neutron source based on the $\text{Be}(p, n)$ reaction using a 30MeV proton cyclotron accelerator.	Applied Radiation and Isotopes	67	S258-S261	2009
K. IIDA-ONISHI, S. KAWABATA, S. MIYATA, T. MASUBUCHI, A. DOI, K. YOKOYAMA, T. KUROIWA, K. ONO, H. KUMADA, M. KIRIHATA, S. MIYATAKE	Evaluation of the Biological Effects of Boron Neutron Capture Therapy for the Human Malignant Meningioma Cell Line IOMM-Lee.	Bulletin of the Osaka Medical College	55 (1)	9-19	2009

N. Nariyama, T. Ohigashi, K. Umetani, K. Shinohara, H. Tanaka, A. Ma ruhashi, G. Ka shino, A. Kuri hara, T. Kondo b, M. Fukumot o, K. Ono	Spectromicroscopic film dosimetry for high-energy microbeam from synchrotron radiation.	Applied Radi ation and Is otopes	67	155-159	2009
S. Haginomori, S. Miyatake, T. Inui, M. Ara ki, S. Kawabat a, A. Takamaki, K. Lee, H. Tak enaka, T. Kuro iwa, V. Uesugi, H. Kumad, K. Ono	PLANNED FRACTIONATED BORON NEUTRON CAPTURE THERAPY USING EPITHERMAL NEUTRONS FOR A PATIENT WITH RECURRENT SQUAMOUS CELL CARCINOMA IN THE TEMPORAL BONE:A CASE REPORT.	HEAD & NECK	31 (3)	412-418	2009
S. Miyatake, S. Kawabata, K. Yokoyama, T. Kuroiwa, H. Michiue, Y. S akurai, H. Kum ada, M. Suzuk i, A. Maruhash i, M. Kirihat a, K. Ono	Survival benefit of Boron neutron capture therapy for recurrent malignant glioma.	J. Neurooncol	91	199-206	2009
S. KAWABATA, S. MIYATAKE, T. KUROIWA, K. YOKOYAMA, A. DOI, K. IIDA, S. MIYATA, N. NONOGUCHI, H. MICHIEU, M. TA KAHASHI, T. IN OMATA, Y. IMAH ORI, M. KIRIHA TA, Y. SAKURA I, A. MARUHASH I, H. KUMADA a nd K. ONO	Boron Neutron Capture Therapy for Newly Diagnosed Glioblastoma.	J. Radiat. R es.,	50	51-60	2009
Fujita Y, Kato I. Iwai S, On o K, Suzuki M, Sakurai Y, Oh nishi K, Ohnis hi T, Yura Y.	Role of p53 mutation in the effect of boron neutron capture therapy on oral squamous cell carcinoma.	Radiat Onco l.	4	63-	2009
Liu Y, Nagata K, Masunaga S, Suzuki M, Kas hino G, Kinash i Y, Tanaka H, Sakurai Y, Ma ruhashi A, Ono K.	Gamma-ray irradiation enhanced boron-10 compound accumulation in murine tumors.	J Radiat Re s.	50 (6)	553-557	2009

Kato I, Fujita Y, Maruhashi A, Kumada H, Ohmae M, Kiriha ta M, Imahori Y, Suzuki M, Sakrai Y, Sumi T, Iwai S, Nakazawa M, Murata I, Miyamaru H, Ono K.	Effectiveness of boron neutron capture therapy for recurrent head and neck malignancies.	Appl Radiat Isot.	67 (7-8 Supp 1)	S37-42	2009
Miyatake S, Kawabata S, Nonoguchi N, Yokoyama K, Kuroiwa T, Matsui H, Ono K.	Pseudoprogression in boron neutron capture therapy for malignant gliomas and meningiomas.	Neuro Oncol.	11 (4)	430-436	2009
川端信司、宮武伸一、宮田至朗、横山邦夫、大西恭子、三木義人、黒岩敏彦、今堀良夫、切畑光統、小野公二	ホウ素中性子捕捉療法による悪性神経膠腫の治療効果 Therapy effects of boron neutron capture therapy for malignant glioma.	定位的放射線治療	13	23~30	2009
川端信司、宮武伸一、黒岩敏彦、小野公二	グリオーマに対する中性子捕捉療法.	脳21	12 (1)	102-107	2009
Tanaka, K., Arao, T., Maegawa, M., Matsumoto, K., Kaneda, H., Kudo, K., Fujita, Y., Yokote, H., Yanagihara, K., Yamada, Y., Okamoto, I., Nakagawa, K., Nishio, K.	SRPX2 is overexpressed in gastric cancer and promotes cellular migration and adhesion.	Int J Cancer	124	1072-1080	2009
Takeda, K., Negoro, S., Tamura, T., Nishiwaki, Y., Kudoh, S., Yokota, S., Matsui, K., Semba, H., Nakagawa, K., Takada, Y., Ando, M., Shibata, T., Saijo, N.	Phase III trial of docetaxel plus gemcitabine versus docetaxel in second-line treatment for non-small-cell lung cancer: results of a Japan Clinical Oncology Group trial (JCOG0104).	Annals of Oncology	20 (5)	835-841	2009

Okabe, T., Okamoto, I., Tsukioka, S., Uchida, J., Hatashita, E., Yamada, Y., Yoshida, T., Nishio, K., Fukuoka, M., Janne, PA., Nakagawa, K.	Addition of S-1 to the epidermal growth factor receptor inhibitor gefitinib overcomes gefitinib resistance in non-small cell lung cancer cell lines with MET amplification.	Clin Cancer Res	15 (3)	907-13	2009
Okamoto, K., Tsurutani, J., Terashima, M., Okamoto, I., Nakagawa, K.	Zoledronic acid-induced regression of multiple metastases at nonskeletal sites.	Ann Oncol	20 (4)	796-7	2009
Yamamoto, N., Sekine, I., Nakagawa, K., Takada, M., Fukuoka, M., Tanigawara, Y., Saijo, N.	A Pharmacokinetic and Dose Escalation Study of Pegfilgrastim (KRN125) in Lung Cancer Patients with Chemotherapy-induced Neutropenia.	Jpn J Clin Oncol	39 (7)	425-30	2009
Tamura, K., Okamoto, I., Ozaki, T., Kashii, T., Takeda, K., Kobayashi, M., Matsui, K., Shibata, T., Kurata, T., Nakagawa, K., Fukuoka, M.	Phase I/II study of S-1 plus carboplatin in patients with advanced non-small cell lung cancer.	Eur J Cancer	45 (12)	2732-7	2009
Shimizu, T., Okamoto, I., Tamura, K., Satoh, T., Miyazaki, M., Akashi, Y., Ozaki, T., Fukuoka, M., Nakagawa, K.	Phase I clinical and pharmacokinetic study of the glucose-conjugated cytotoxic agent D: -19575 (glufosfamide) in patients with solid tumors.	Cancer Chemother Pharmacol	65	243-250	2009
Kurata, T., Kashii, T., Takeda, K., Seki, N., Tsuboi, M., Kobayashi, M., Satoh, T., Nakagawa, K., Fukuoka, M.	A phase I study of topotecan plus carboplatin for relapsed SCLC: WJTOG trial.	J Thorac Oncol	4 (5)	644-8	2009

Satoh, T., Okamoto, I., Miyazaki, M., Morinaga, R., Tsuya, A., Hasegawa, Y., Terashima, M., Ueda, S., Fukuoka, M., Ariyoshi, Y., Saito, T., Masuda, N., Watanabe, H., Taguchi, T., Kakiyama, T., Aoyama, Y., Hashimoto, Y., Nakagawa, K.	Phase I study of YM155, a novel survivin suppressant, in patients with advanced solid tumors.	Clin Cancer Res	15 (11)	3872-80	2009
Nakagawa, K., Minami, H., Kanezaki, M., Mukaiyama, A., Minamide, Y., Uejima, H., Kurata, T., Nogami, T., Kawada, K., Mukai, H., Sasaki, Y., Fukuoka, M.	Phase I dose-escalation and pharmacokinetic trial of Lapatinib (GW572016), a selective oral dual inhibitor of ErbB-1 and -2 tyrosine kinases, in Japanese patients with solid tumors.	Jpn J Clin Oncol	39 (2)	116-123	2009
Takezawa, K., Okamoto, I., Yonesaka, K., Hatashita, E., Yamada, Y., Fukuoka, M., Nakagawa, K.	Sorafenib inhibits non-small cell lung cancer cell growth by targeting B-RAF in KRAS wild-type cells and C-RAF in KRAS mutant cells.	Cancer Res	69 (16)	6515-21	2009
Iwasa, T., Okamoto, I., Suzuki, M., Hatashita, E., Yamada, Y., Fukuoka, M., Ono, K., Nakagawa, K.	Inhibition of Insulin-Like growth factor 1 receptor by CP-751,871 radiosensitizes Non-Small cell lung cancer cells.	Clin Cancer Res	15 (16)	5117-25	2009
Sekine, I., Ichinose, Y., Nishiwaki, Y., Yamamoto, N., Tsuboi, M., Nakagawa, K., Shinkai, T., Negoro, S., Imamura, F., Eguchi, K., Takeda, K., Itoh, Y., Tamura, T., Saijo, N., Fukuoka, M.	Quality of life and disease-related symptoms in previously treated Japanese patients with non-small-cell lung cancer: results of a randomized phase III study (V-15-32) of gefitinib versus docetaxel.	Annals of Oncology	20 (9)	1483-1488	2009

Okamoto, K., Okamoto, I., Takezawa, K., Tachibana, I., Fukuoka, M., Nishimura, Y., Nakagawa, K.	Cisplatin and Etoposide Chemotherapy Combined with Early Concurrent Twice-daily Thoracic Radiotherapy for Limited-disease Small Cell Lung Cancer in Elderly Patients.	Jpn J Clin Oncol	40 (1)	54-59	2009
Kunitoh, H., Tamura, T., Shibata, T., Nakagawa, K., Takeida, K., Nishiwaki, Y., Osaki, Y., Noda, K., Yokoyama, A., Saijo, N; JCOG Lung Cancer Study Group Tokyo Japan.	A phase-II trial of dose-dense chemotherapy in patients with disseminated thymoma: report of a Japan Clinical Oncology Group trial (JCOG 9605).	Br J Cancer	101 (9)	1549-54	2009
Hayashi, H, Okamoto, I., Ichikawa, Y., Miyazaki, M., Yoshioka, H., Kunimasa, K., Nakagawa, K.	Retreatment of recurrent malignant pleural mesothelioma with cisplatin and pemetrexed. International	Journal of Clinical Oncology		Published online	March 2010
Takashi Nakano	A feasibility study of induction pemetrexed plus cisplatin followed by extrapleural pneumonectomy and postoperative hemithoracic radiation for malignant	Jpn J Clin Oncol	39	186-188	2009
Takashi Nakano	Possible involvement of caspase-6 and -7 but not caspase-3 in the regulation of hypoxia-induced apoptosis in tube-forming endothelial cells.	Exp Cell Res.	315	327-335	2009
Takashi Nakano	Osteopontin modulates malignant pleural mesothelioma cell functions in vitro.	Anticancer Research	29	2205-2214	2009
Takashi Nakano	Impairment in cytotoxicity and expression of NK cell-activating receptors on human NK cells following exposure to asbestos fibers.	International Journal of Immunopathology and Pharmacology	22	579-590	2009

Takashi Nakano	All-trans-retinoic acid inhibits tumor growth of malignant pleural mesothelioma in mice.	Eur Respr J.	34	1159-1167	2009
Takashi Nakano	Tuning of apoptosis-mediator gene transcription in HepG2 human hepatoma cells through an adenosine signal.	Cancer Lett	291	225-229	2009
Oda T et al.	Tumorigenic role of orphan nuclear receptor NROB1 in lung adenocarcinoma.	American Journal of Pathology	175	1235	2009
Ikeda J et al.	Expression of CUB domain containing protein (CDCP1) is correlated with prognosis and survival of patients with adenocarcinoma of lung.	Cancer Science	100	429	2009
平塚純一, 粟飯原輝 人, 小野 公二	【粒子線治療の普及に向けた課題と展望】ホウ素中性子捕捉療法 (BNCT) の現状と可能性さらなる展開に向けた課題はなにか (解説/特集)	DIGITAL MEDICINE	7巻 6号	28- 30	2009
Feng B, Tomizawa K, Michiue H, Miyatake S, Han XJ, Fujimura A, Seno M.	Delivery of sodium borocaptate to glioma cells using immunoliposome conjugated with anti-EGFR antibodies by ZZ-His.	Biomaterials	30 (9),	1746-1755	2009
Tanimori S, Nishimura T, Kirihata M.	Synthesis of novel quinoxaline derivatives and its cytotoxic activities.	Bioorg Med Chem Lett.	19 (15)	4119-4121	2009

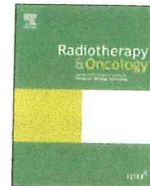


ELSEVIER

Contents lists available at ScienceDirect

Radiotherapy and Oncology

journal homepage: www.thegreenjournal.com



Original article

Impact of accelerator-based boron neutron capture therapy (AB-BNCT) on the treatment of multiple liver tumors and malignant pleural mesothelioma

Minoru Suzuki^{a,*}, Hiroki Tanaka^b, Yoshinori Sakurai^b, Genro Kashino^a, Liu Yong^a, Shinichiro Masunaga^a, Yuko Kinashi^a, Toshinori Mitsumoto^c, Satoru Yajima^c, Hiroshi Tsutsui^c, Takemi Sato^c, Akira Maruhashi^b, Koji Ono^a

^a Particle Radiation Oncology Research Center, Research Reactor Institute, Kyoto University, Osaka, Japan

^b Radiation Medical Physics Laboratory, Research Reactor Institute, Kyoto University, Osaka, Japan

^c Sumitomo Heavy Industries, Ltd., Tokyo, Japan

ARTICLE INFO

Article history:

Received 14 October 2008

Received in revised form 9 January 2009

Accepted 11 January 2009

Available online xxxx

Keywords:

Accelerator-based neutron source

Boron neutron capture therapy

Liver tumor

Malignant pleural mesothelioma

ABSTRACT

Background and purpose: To confirm the feasibility of accelerator-based BNCT (AB-BNCT) for treatment of multiple liver tumors and malignant pleural mesothelioma (MPM), we compared dose distribution and irradiation time between AB-BNCT and reactor-based BNCT (RB-BNCT).

Material and methods: We constructed treatment plans for AB-BNCT and RB-BNCT of four multiple liver tumors and six MPM. The neutron beam data on RB-BNCT were those from the research reactor at Kyoto University Research Reactor Institute (KURRI). The irradiation time and dose–volume histogram data were assessed for each BNCT system.

Results: In BNCT for multiple liver tumors, when the 5 Gy-Eq dose was delivered as the mean dose to the healthy liver tissues, the mean dose delivered to the liver tumors by AB-BNCT and RB-BNCT was 68.1 and 65.1 Gy-Eq, respectively. In BNCT for MPM, when the mean lung dose to the normal ipsilateral lung was 5 Gy-Eq, the mean dose delivered to the MPM tumor by AB-BNCT and RB-BNCT was 20.2 and 19.9 Gy-Eq, respectively. Dose distribution analysis revealed that AB-BNCT is superior to RB-BNCT for treatment of deep-seated tumors.

Conclusions: The feasibility of the AB-BNCT system constructed at our institute was confirmed from a clinical viewpoint in BNCT for multiple liver tumors and MPM.

© 2009 Published by Elsevier Ireland Ltd. Radiotherapy and Oncology xxx (2009) xxx–xxx

Boron neutron capture therapy (BNCT) is based on a nuclear reaction: non-radioactive isotope ^{10}B atoms that have absorbed low energy (<0.5 eV) neutrons disintegrate into alpha (^4He) particles and recoiled lithium nuclei (^7Li). These particles deposit large energy along their very short paths (<10 μm), whose lengths are equal to or shorter than a typical cell size [1,2]. Malignant cells with ^{10}B are thus destroyed following thermal neutron irradiation by these high linear energy (LET) particles. If a sufficient number of ^{10}B atoms accumulate in the tumor cells and the gradient of the ^{10}B concentrations between the tumor and the surrounding normal tissues is large, then boron neutron capture irradiation will be selectively delivered to the tumor.

Selective high LET particle irradiation to cancer cells is a unique property of BNCT, which is an advantage over other radiotherapy modalities. For the use of this unique property, we have continued

preclinical studies on application of BNCT to tumors located in radiosensitive organs, such as liver and lung [3,4]. In our previous studies, the feasibility of BNCT for treating multiple liver tumors and inoperable malignant pleural mesothelioma (MPM) was confirmed from the viewpoint of dose distribution [5,6]. Based on these preclinical studies, we have carried out clinical BNCT for multiple liver tumors and MPM since 2005 at Kyoto University Research Reactor Institute (KURRI). One patient with asbestos-induced MPM and three cases of multiple liver tumors have already been treated with BNCT [7,8].

To deal with the increasing number of candidates for BNCT, development of an accelerator-based BNCT (AB-BNCT) system is a prerequisite. Construction of an AB-BNCT system at KURRI was started in June 2008 and was finished in December 2008. To prepare the protocol for clinical studies using the AB-BNCT system, comparison of the parameters for dose distribution and irradiation time between Kyoto University reactor (KUR)-based BNCT (RB-BNCT) and the AB-BNCT is needed. The aim of the present study was to investigate the advantages of AB-BNCT over RB-BNCT for multiple liver tumors and MPM.

* Corresponding author. Address: Particle Radiation Oncology Research Center, Research Reactor Institute, Kyoto University, 2-1010, Asashiro-nishi, Kumatori-cho, Sennan-gun, Osaka 590-0494, Japan.

E-mail address: msuzuki@rri.kyoto-u.ac.jp (M. Suzuki).

Material and methods

Accelerator

Our AB-BNCT system consists of a cyclotron accelerator that produces a proton beam of ~ 2 mA at 30 MeV, beam transport system, beam scanning system on the beryllium target, target cooling system, neutron-beam-shaping assembly (BSA), multileaf collimator, and an irradiation bed for patients in both sitting and decubitus positions. Fig. 1 shows a schematic layout of the BSA for production of epi-thermal neutrons.

The Li(p,n) reaction at low proton energy is widely accepted as the most promising for epi-thermal neutron generation [9]. However, we selected the Be(p,n) reaction with 30 MeV for our AB-BNCT system because: (1) the system using Li(p,n) reaction needs an accelerator with a current of >5 mA to yield an intensity of epi-thermal neutron flux of 1×10^9 n/cm²/s. No accelerator is presently available to achieve such a high current; (2) it is difficult to stably operate a lithium target with heat >10 kW because the 180 °C melting point of lithium is much lower than that of beryllium, which is 1278 °C; and (3) the Be(p,n) reaction with 30 MeV has a higher neutron yield compared with the Li(p,n) reaction. The neutron yield of the Li(p,n) reaction with 1.9 MeV (near threshold) is about 2.4×10^{-6} (neutrons/proton) [9]. Whereas, the neutron yield of the Be(p,n) reaction with 30 MeV is about 3.0×10^{-2} (neutrons/proton) [10].

The reaction of a proton with the beryllium target emits high energy neutrons at up to 28 MeV in the 0° direction. The 0° neutron yield is the largest. The BSA consists of lead, iron, calcium fluoride, and aluminum for reducing neutron energy and shaping an epi-thermal neutron beam. The BSA is surrounded by polyethylene material for shielding fast neutrons and for decreasing radiation to the patient's body. The γ -ray dose contamination in the treatment neutron beam increases because of γ -rays coming from the neutron capture in hydrogen materials such as polyethylene. How-

ever, the γ -ray dose contamination per epi-thermal neutron in a treatment beam under free-air conditions is 7.75×10^{-14} Gy cm² (epi-thermal region is from 0.5 eV to 40 keV). This value is sufficiently below than the IAEA-TECDOC-1223 target value of 2×10^{-13} [11].

KUR

KUR is a light water-moderated, tank-type nuclear research reactor, with a nominal power of 5 MW. The Heavy Water Neutron Irradiation Facility (HWNIF) is a bio-medical facility at KUR-RI. The facility has been previously described in detail [12,13]. The higher energy neutrons are moderated by the epi-thermal neutron moderator, which is the mixture of aluminum and heavy water (80%/20% in volume). The heavy-water spectrum shifter is installed outside of the epi-thermal neutron moderator, for control of the neutron-energy spectrum. The total heavy-water thickness can be changed from 0 to 90 cm in 10-cm increments. The thermal neutron filters of cadmium and boral are installed outside of the spectrum shifter, to regulate the thermal neutron component. The apertures of these filters are changed from 0 to 62 cm. Outside of the filters, the bismuth layer is placed for γ -ray elimination. In this facility, neutron beams with various energy spectra from almost pure thermal to epi-thermal are available by controlling the heavy-water thickness in the spectrum shifter, and by the opening and closing of the cadmium and boral thermal neutron filters.

Comparison of neutron spectra

A comparison has been carried out between the neutron spectra at the output port in air for AB-BNCT and RB-BNCT. For the KUR, the neutron spectrum was measured by activation of gold foils. For the accelerator-based neutron source, the neutron spectrum was obtained by simulations from a calculated neutron source.

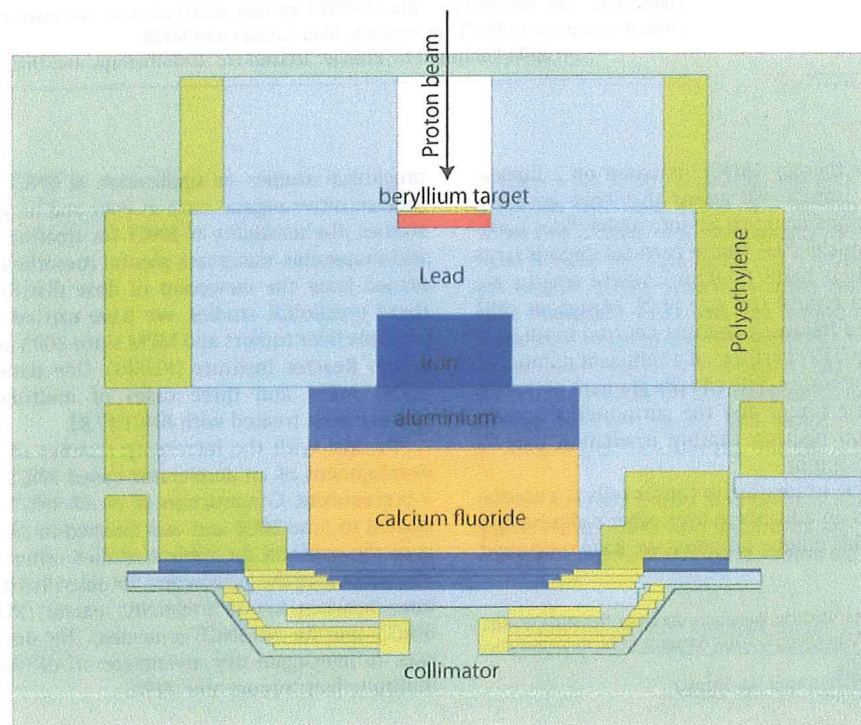


Fig. 1. Schematic layout of BSA for production of epi-thermal neutrons based on beryllium (p,n) reaction using 30 MeV proton beam.

Assumption and parameters for BNCT treatment planning

The conditions and parameters in BNCT treatment planning are summarized in Table 1. The parameters were approximately the same as those in our previous treatment planning studies on BNCT for multiple liver tumors and MPM [5,6]. The details for determination of each parameter have been described in our previous reports [5,6]. The compound biologic effectiveness (CBE) factors of the boron compounds in Table 1 were requested to convert the physical dose of BNCT to the photon-equivalent dose (Gy-Eq) and the relative biologic effectiveness (RBE) of each component of the beam. The CBE factors were used as an alternative RBE in evaluating the biologically equivalent absorbed dose by BNCT. This was because the same or different boron compounds might yield variable effects on different tissues, as a result of variations in the microdistribution of the boron compounds and the morphological character of the target cells. The CBE factors and RBE values for the tumors were the same as those used in clinical BNCT trials [14,15]. The CBE factors and RBE values for liver and lung were determined by experimental studies using rodents [16,17]. We adopted the value of 3.0 as the RBE value of $^{14}\text{N}(\text{n},\text{p})\ ^{14}\text{C}$ radiations and fast neutrons for liver. The value was greater than the RBE of fast neutron for hepatocytes reported by Ono et al. [18]. Use of the greater RBE for normal liver is expected to decrease the occurrence of radiation-induced liver disease in clinical situation.

The difference in the method between BNCT for multiple liver tumors and MPM was the drug delivery system (DDS) for the boron compounds. In BNCT for multiple liver tumors, borocaptate sodium (BSH), which has been employed as a boron compound in clinical BNCT trials for malignant glioma, was administered via the hepatic artery with vessel occlusion materials (lipiodol), according to our previous reports [3,5,7]. This DDS method is possible to deliver ^{10}B to liver tumors, that are highly selective [3]. In the present study, ^{10}B tumor/liver concentration ratio was assumed to be 20 according to our present study (Table 1) [3]. In BNCT for MPM, boronophenylalanine (BPA), another boron compound available in clinical trials, was administered intravenously [8]. In the MPM cases, ^{10}B tumor/lung or liver concentration ratio was assumed to be 3.5 (Table 1).

In BNCT for multiple liver tumors, the whole liver was defined as the clinical target volume (CTV). Three-port irradiation by anterior, right and posterior (ARP) beams was planned to deliver thermal neutrons to whole liver as homogeneously as possible [5]. Because the CTV for MPM was defined as the hemithorax, including the tumor and ipsilateral normal lung, the CTV was divided into upper and lower portions because of the limit in circular collimator size (maximum 25 cm). Each CTV was irradiated with anterior-

posterior (AP) beams or 20–30° anterior-oblique and posterior-oblique beams. The oblique beams were used to deliver greater doses to the tumors at mediastinal side compared to AP beams in some cases. Four-port irradiation was needed for covering the whole CTV.

Overview of BNCT treatment planning using the simulation environment for radiotherapy applications (SERA) system

Computed tomography (CT) images of four patients with multiple liver tumors and six with MPM were used in the present study. Three patients had right MPM, and the other three had left MPM. In four BNCT treatment plans for multiple liver tumors, a total of 11 liver tumors were evaluated.

We have already reported the treatment planning studies on BNCT for multiple liver tumors and MPM using KUR epi-thermal neutron beam data and the SERA system, a currently available BNCT treatment planning system. Details of the procedures in treatment planning using the SERA system have been described in our previous reports [5,6].

Dose–volume histogram (DVH) analysis

The SERA system can provide DVH data for each tumor or for the normal tissues as a whole. The maximum, minimum and mean doses to the tumors and normal tissues were assessed for each case. In radiotherapy for liver tumors and MPM, radiation-induced liver injury and radiation pneumonitis are dose-limiting toxicities, therefore, we set the doses delivered to normal liver and lung tissues as constraint doses. In the present study, 5.0 Gy-Eq of the mean liver and lung doses were set as the constraint doses. Under these conditions, each DVH parameter and irradiation time was compared between AB-BNCT and RB-BNCT. The doses delivered to the tumors with AB-BNCT and RB-BNCT were compared by means of Wilcoxon's signed-rank test.

Results

Neutron spectra comparison

Fig. 2 shows the neutron spectra at the output port produced by the accelerator-based neutron beam (1 mA, 30 MeV proton beam with the beryllium target) and epi-thermal neutron beam of HWNIF in the KUR. The neutron beam produced by the accelerator was harder compared with that of the KUR. In comparison of the maximum numbers yielded per lethargy, the accelerator source produced neutrons approximately four orders of magnitude higher than KUR.

Comparison of dose distributions in BNCT for multiple liver tumors

Table 2 summarizes the DVH parameters for tumor and normal liver and irradiation time for three-port irradiation in AB-BNCT and RB-BNCT for multiple liver tumors. To compare irradiation time and dose distribution in tumors between AB-BNCT and RB-BNCT, all treatment plans were normalized to deliver mean doses of 5 Gy-Eq to the whole liver. The average irradiation time was 43.8 and 198.3 min in AB-BNCT and RB-BNCT, respectively. The averages of the maximum, mean and minimum doses delivered to all 11 tumors in the AB-BNCT were significantly higher than those in RB-BNCT (78.7 vs. 77.4 Gy-Eq, 68.1 vs. 65.1 Gy-Eq and 57.7 vs. 53.7 Gy-Eq, $p = 0.0023$, $p = 0.0040$, and $p = 0.0022$, respectively).

Fig. 3A shows the isodose distributions in the representative case with deep-seated liver tumor provided by RB-BNCT and AB-BNCT. AB-BNCT delivered higher dose to the tumor than RB-BNCT. Fig. 3B shows the depth–dose distribution profiles along the right

Table 1

^{10}B concentrations and RBE and CBE factors used for conversion of physical dose (Gy) to photon-equivalent dose (Gy-Eq).

	Liver tumor MPM		Liver	Lung
^{10}B concentration (ppm)	200.0	84.0	10.0 (Liver tumor cases) 24.0 (MPM cases)	24.0
RBE, CBE				
$^{10}\text{B}(\text{n},\alpha)\ ^7\text{Li}$	2.5	3.8 (CBE _{for BPA})	0.94 (CBE _{for BSH}) 4.25 (CBE _{for BPA}) [†]	2.3 (CBE _{for BPA}) [†]
$^{14}\text{N}(\text{n},\text{p})\ ^{14}\text{C}$	3.0	3.0	3.0	2.2 [†]
Fast neutron	3.0	3.0	3.0	2.2 [†]
γ -Ray	1.0	1.0	1.0	1.0

Abbreviations: RBE = relative biological effectiveness; CBE = compound biological effectiveness; MPM = malignant pleural mesothelioma; BSH = borocaptate sodium; BPA = boronophenylalanine.

[†] Data from Suzuki et al. [16].

[†] Data from Kiger et al. [17].

Please cite this article in press as: Suzuki M et al. Impact of accelerator-based boron neutron capture therapy (AB-BNCT) on the treatment of multiple liver tumors and malignant pleural mesothelioma. Radiother Oncol (2009), doi:10.1016/j.radonc.2009.01.010

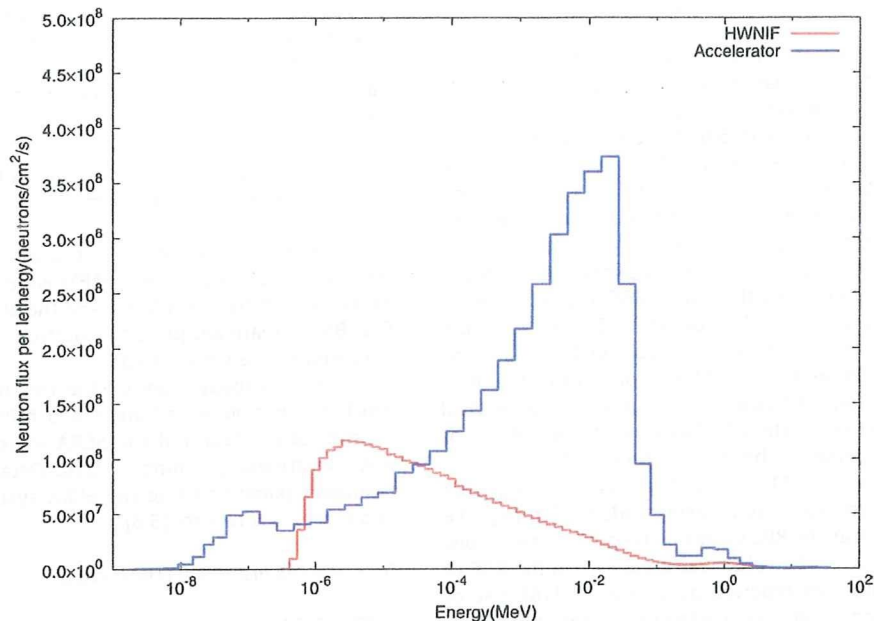


Fig. 2. Comparison of neutron spectrum between HWNIF and accelerator-based neutron source shaped with the BSA.

neutron beam axis which passed into the deep-seated liver tumor. The depth-dose profiles in the tumor located at a depth of 9.0–12.5 cm demonstrated that AB-BNCT delivered a higher dose than RB-BNCT. Fig. 3C shows the depth-ratio of thermal neutron fluence-rate (AB-BNCT to RB-BNCT) profiles along the same beam axis as in Fig. 3B. The ratio of thermal neutron fluence-rate increased from 3.9 to 6.3 at a depth of 1–12 cm, which was caused by the property of the accelerator-based neutron source which has a peak at higher energy in its neutron spectrum compared with that of the KUR as shown in Fig. 2.

Comparison of treatment parameters in BNCT for MPM

Table 3 compares the DVH parameters for tumor and normal lung and irradiation time for four-port irradiation in AB-BNCT and RB-BNCT for MPM. To compare irradiation time and dose distribution in the tumor between AB-BNCT and RB-BNCT, all treatment plans were normalized to deliver mean doses of 5 Gy-Eq to the whole of the ipsilateral lung. The average irradiation time in AB-BNCT and RB-BNCT were 29.9 and 134.7 min, respectively. The mean doses delivered to the MPM tumors by AB-BNCT and RB-BNCT were 20.2 and 19.9 Gy-Eq, respectively. The average of the maximum doses delivered to the MPM tumors by AB-BNCT was significantly lower than those with RB-BNCT (36.4 vs. 40.0 Gy-Eq, $p = 0.0253$). On the other hand, the average of the minimum doses delivered to the MPM tumors by AB-BNCT was significantly higher than those with RB-BNCT (4.6 vs. 4.3 Gy-Eq, $p = 0.0275$).

Fig. 4A shows the isodose distributions for the tumor in the representative case with MPM provided by RB-BNCT and AB-BNCT. AB-BNCT delivered higher dose to the MPM tumor located in the middle of the thorax compared to RB-BNCT. Fig. 4B shows the depth-dose distribution profiles along the anterior epi-thermal neutron beam axis in the case of MPM. The tumor located at a depth of 9.0–12.5 cm received a greater dose with AB-BNCT compared with RB-BNCT. On the other hand, RB-BNCT delivered a greater dose to the tumor located at a depth of 3.5–5.0 cm. Fig. 4C shows the depth-thermal neutron flux ratio (AB-BNCT to RB-BNCT) profiles along the same beam axis as Fig. 4B. The thermal neutron flux ratio increased from 4.0 to 5.8 within a depth of 1–12 cm.

Discussion

In BNCT for multiple liver tumors and MPM, the most important feature of the AB-BNCT system at our institute is capability to deliver three- or four-port irradiation within a reasonable treatment time (<1 h), including the time required for changing patient position. Shortening of irradiation time makes it possible to finish irradiation while maintaining a high ^{10}B concentration in the tumor, and to reduce the non-selective background dose. In addition, shortening of irradiation time provides comfort to the patients during irradiation and single or two-fractionated BNCT has economic benefits.

Another important feature of the AB-BNCT system is its capability of delivering greater doses to deep-seated tumors than RB-

Table 2
Irradiation time and DVH parameters showing averages (with range) for liver tumors and normal liver.

Neutron source	Irradiation time (min)	Tumor			Liver		
		D_{\max} (Gy-eq)	D_{mean} (Gy-eq)	D_{\min} (Gy-eq)	D_{\max} (Gy-eq)	D_{mean} (Gy-eq)	D_{\min} (Gy-eq)
KUR	198.3 (177.0–216.8)	77.4 (49.3–104.6)	65.1 (33.8–84.2)	53.7 (20.7–76.5)	6.9 (6.4–7.4)	5.0*	1.9 (1.3–2.1)
Accelerator	43.8 (39.0–47.8)	78.7 (52.6–102.0)	68.1 (37.7–87.1)	57.7 (23.6–76.7)	6.7 (6.3–7.2)	5.0*	1.7 (1.1–2.2)

Abbreviations: DVH = dose-volume histogram; KUR = Kyoto University Research Reactor.

* The mean dose to the liver normalized to 5.0 Gy-Eq.

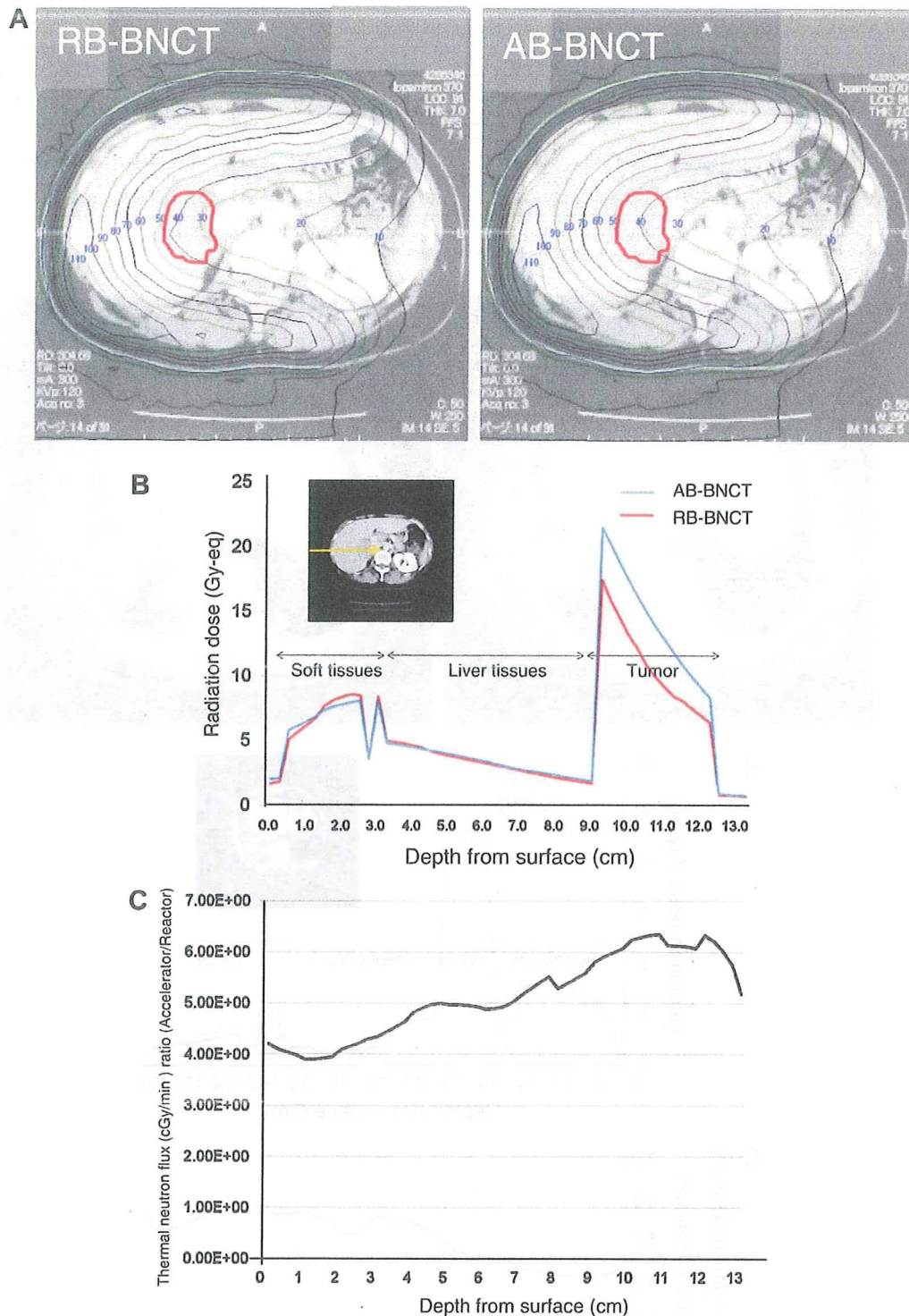


Fig. 3. (A) Comparison of isodose distribution between RB-BNCT and AB-BNCT. The liver tumor is contoured with a solid red line. (B) Depth-dose distribution profiles along the right neutron beam axis, which passed into the deep-seated liver tumor located at a depth of 9.5–12.5 cm. A yellow arrow on the CT image indicates the beam axis. (C) Depth-thermal neutron flux ratio (AB-BNCT to RB-BNCT) profiles along the same beam axis as that in (B).

BNCT, under conditions in which the mean doses delivered to normal liver or lung are equal. This advantage of AB-BNCT over RB-BNCT was especially evident in BNCT for deep-seated multiple liver tumors. As shown in Table 2, AB-BNCT delivered significantly greater doses to liver tumors than RB-BNCT did. As shown in Fig. 2, the AB-BNCT system provided a higher peak energy (near 10 keV) in its neutron spectrum compared with RB-BNCT. The

higher energy peak of the AB-BNCT system is well suited for generating a thermal neutron flux distribution suitable for deep-seated tumors and provides a larger thermal neutron fluence to areas deep within the body compared to the RB-BNCT system. However, while the epi-thermal neutron beam of HWNIF in the KUR has a softer spectrum and the near-10-keV component is not significant, the higher epi-thermal neutron component in-

Table 3
Irradiation time and DVH parameters showing averages (with range) for MPM tumors and normal lung.

Neutron source	Irradiation time (min)	Tumor			Ipsilateral lung			Contralateral lung			Liver*		
		D_{max} (Gy-eq)	D_{mean} (Gy-eq)	D_{min} (Gy-eq)	D_{max} (Gy-eq)	D_{mean} (Gy-eq)	D_{min} (Gy-eq)	D_{max} (Gy-eq)	D_{mean} (Gy-eq)	D_{min} (Gy-eq)	D_{max} (Gy-eq)	D_{mean} (Gy-eq)	D_{min} (Gy-eq)
KUR	134.7 (117.4–156.4)	40.0 (35.0–42.3)	19.9 (19.3–20.7)	4.3 (3.0–6.1)	7.7 (7.1–8.1)	5.0 [†]	2.2 (1.8–2.5)	5.3 (4.7–6.8)	1.4 (1.2–1.9)	0.4 (0.3–0.6)	10.4 (10.0–10.8)	5.0 (4.6–5.2)	0.9 (0.8–1.0)
Accelerator	29.9 (26.3–33.3)	36.4 (33.0–38.3)	20.2 (19.7–21.0)	4.6 (3.4–6.4)	7.3 (6.9–7.5)	5.0 [†]	2.3 (1.8–2.6)	4.9 (4.2–6.0)	1.3 (1.1–1.8)	0.3 (0.2–0.5)	9.7 (9.2–10.2)	5.0 (4.7–5.2)	0.8 (0.7–0.8)

Abbreviations: DVH = dose-volume histogram; MPM = malignant pleural mesothelioma; KUR = Kyoto University Research Reactor.

* The average (range) of DVH data for liver was estimated using the data for three cases with right MPM.

[†] The mean dose to the liver normalized to 5.0 Gy-Eq.

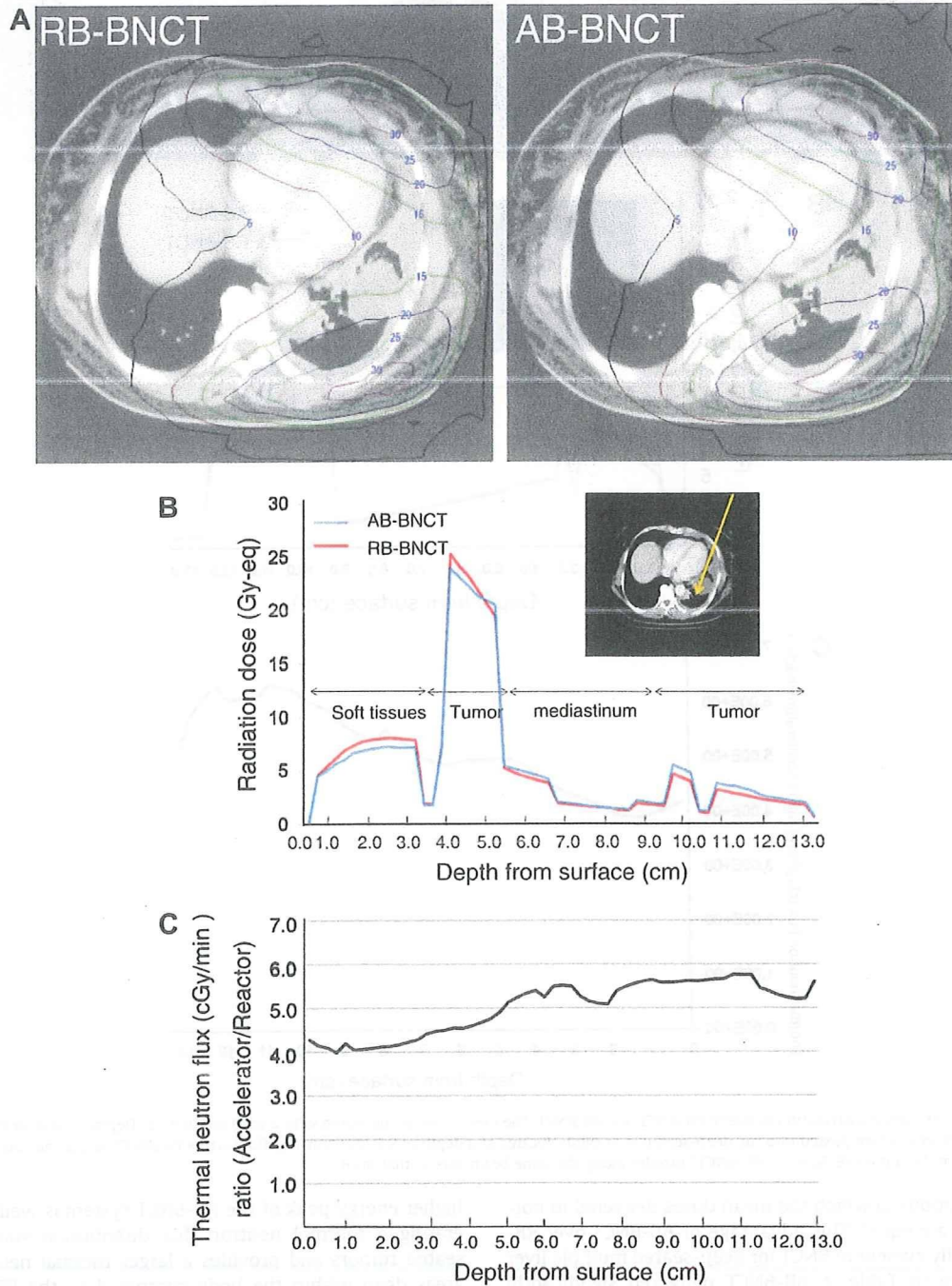


Fig. 4. (A) Comparison of isodose distribution between RB-BNCT and AB-BNCT. (B) Depth-dose distribution profile along the anterior-oblique neutron beam axis in the case of BNCT for MPM. A yellow arrow on the CT image indicates the beam axis. (C) Depth-thermal neutron flux ratio (AB-BNCT to RB-BNCT) profiles along the same beam axis as that in (B).